Since January 2020 Elsevier has created a COVID-19 resource centre with free information in English and Mandarin on the novel coronavirus COVID-19. The COVID-19 resource centre is hosted on Elsevier Connect, the company's public news and information website.

Biomedicine & Pharmacotherapy 149 (2022) 112802

Contents lists available at ScienceDirect

Biomedicine & Pharmacotherapy

journal homepage: www.elsevier.com/locate/biopha

Potential inhibitor for blocking binding between ACE2 and SARS-CoV-2 spike protein with mutations

Ming-Shao Tsai [a,b], Wei-Tai Shih [c], Yao-Hsu Yang [c,d], Yu-Shih Lin [e], Geng-He Chang [a,b,f], Cheng-Ming Hsu [a,b], Reming-Albert Yeh [a], Li-Hsin Shu [c], Yu-Ching Cheng [a,c], Hung-Te Liu [c], Yu-Huei Wu [g], Yu-Heng Wu [h], Rou-Chen Shen [a], Ching-Yuan Wu [c,d,i,*]

[a] Department of Otolaryngology, Chang Gung Memorial Hospital, Chiayi, Taiwan
[b] Faculty of Medicine, College of Medicine, Chang Gung University, Tao-Yuan, Taiwan
[c] Department of Chinese Medicine, Chiayi Chang Gung Memorial Hospital, Chiayi, Taiwan
[d] School of Chinese Medicine, College of Medicine, Chang Gung University, Tao-Yuan, Taiwan
[e] Department of Pharmacy, Chiayi Chang Gung Memorial Hospital, Chiayi, Taiwan
[f] Health Information and Epidemiology Laboratory, Chang Gung Memorial Hospital, Chiayi, Taiwan
[g] Department of Biomedical Sciences, Chang Gung University, Tao-Yuan, Taiwan
[h] Department of Electrical Engineering, National Sun Yat-Sen University, Kaohsiung, Taiwan
[i] Research Center for Chinese Herbal Medicine, College of Human Ecology, Chang Gung University of Science and Technology, Taoyuan, Taiwan

ARTICLE INFO

Keywords:
SARS-CoV-2
Spike protein
GB-1
Glycyrrhizic acid
COVID-19

Chemical compounds studied in this article:
Glycyrrhizic acid (Pubchem CID: 14982)
(+)-Catechin (Pubchem CID: 9064)

ABSTRACT

At the time of writing, more than 440 million confirmed coronavirus disease 2019 (COVID-19) cases and more than 5.97 million COVID-19 deaths worldwide have been reported by the World Health Organization since the start of the outbreak of the pandemic in Wuhan, China. During the COVID-19 pandemic, many variants of SARS-CoV-2 have arisen because of high mutation rates. N501Y, E484K, K417N, K417T, L452R and T478K in the receptor binding domain (RBD) region may increase the infectivity in several variants of SARS-CoV-2. In this study, we discovered that GB-1, developed from Chiehyuan herbal formula which obtained from Tian Shang Sheng Mu of Chiayi Puzi Peitian Temple, can inhibit the binding between ACE2 and RBD with Wuhan type, K417N-E484K-N501Y and L452R-T478K mutation. In addition, GB-1 inhibited the binding between ACE2 and RBD with a single mutation (E484K or N501Y), except the K417N mutation. In the compositions of GB-1, glycyrrhizic acid can inhibit the binding between ACE2 and RBD with Wuhan type, except K417N-E484K-N501Y mutation. Our results suggest that GB-1 could be a potential candidate for the prophylaxis of different variants of SARS-CoV-2 infection because of its inhibition of binding between ACE2 and RBD with different mutations (L452R-T478K, K417N-E484K-N501Y, N501Y or E484K).

1. Introduction

At the time of writing, more than 440 million confirmed coronavirus disease 2019 (COVID-19) cases and more than 5.97 million COVID-19 deaths worldwide have been reported by the World Health Organization since the start of the outbreak of the pandemic in Wuhan, China. When severe acute respiratory syndrome coronavirus 2 (SARS-CoV-2) infects a host cell, SARS-CoV-2 spike protein can bind with the host angiotensin-converting enzyme 2 (ACE2) and be primed by host transmembrane protease serine 2 (TMPRSS2) [1]. This step can induce the immune response from the host and generates antibodies to neutralized SARS-CoV-2. Therefore, SARS-CoV-2 spike protein is an important target for COVID-19 prophylaxis, treatment, and vaccines. The receptor binding domain (RBD) in the distal part of the S1 subunit of SARS-CoV-2 spike protein directly binds to the peptidase domain of ACE2 [2,3]. Moreover, human ACE2 can directly contact Gln498, Thr500, Asn501, Lys417, and Tyr453 residues of the amino terminus (N) of the RBD [2]. SARS-CoV-2 is an RNA virus, and RNA viruses have higher mutation rates than other viruses [4,5]. The mutation of residues in the RBD can change the viral infectivity and antigenicity of SARS-CoV-2 [5].

Abbreviations: ACE2, angiotensin converting enzyme 2; SARS-CoV-2, The severe acute respiratory syndrome coronavirus 2; COVID-19, coronavirus disease 2019; RBD, receptor binding domain.

* Correspondence to: Department of Traditional Chinese Medicine, Chang Gung Memorial Hospital, Chiayi Branch, Putzu, Taiwan.
E-mail addresses: smbepigwu77@gmail.com, smbepig@adm.cgmh.org.tw (C.-Y. Wu).

https://doi.org/10.1016/j.biopha.2022.112802
Received 25 January 2022; Received in revised form 3 March 2022; Accepted 7 March 2022
Available online 9 March 2022

Investigations of the function of these mutations in SARS-CoV-2 spike protein are important for the development of treatments.

During the COVID-19 pandemic, many variants of SARS-CoV-2 have arisen because of high mutation rates. Among these variants, variants of concern (VOCs) have shown increased transmissibility, more severe disease, or decreased effectiveness of current diagnostics, vaccines, and treatments [6]. These VOCs usually share similar mutation sites in SARS-CoV-2. The Alpha variant, Gamma variant, and Beta variant

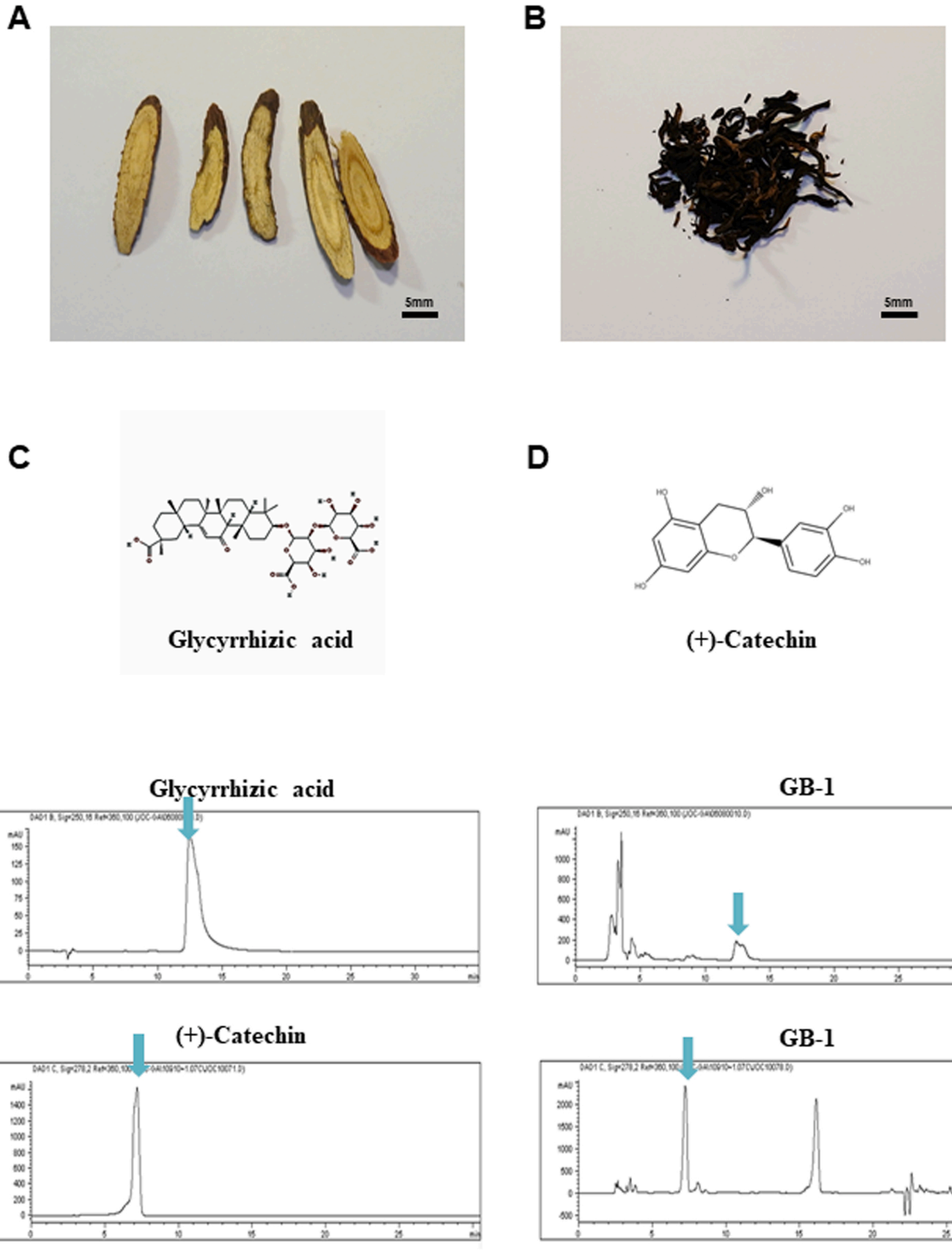

Fig. 1. Identification of reference compounds in GB-1 by HPLC analysis. (A) The photo of the slices of dry root of *Glycyrrhiza uralensis*. (B) The photo of the dry leaves of *Camellia sinensis*. (C) The structure of glycyrrhizic acid. (D) The structure of (+)-catechin. (E) HPLC chromatograms of glycyrrhizic acid and GB-1. (F) HPLC chromatograms of (+)-catechin and GB-1.

linages have the same N501Y mutation, which increases transmissibility through increased binding with ACE2. The E484K mutation, which decreases the in vitro efficacy of neutralizing antibodies [7,8], was found in both Beta variant and Gamma variant [6,9]. Moreover, these accumulations of mutations in different SAR-CoV-2 variants decrease certain efficacy, including those regarding diagnosis, antibody treatment, and vaccines. Alpha variant and Beta variant, which share the N501Y mutation, have higher transmission than other variants [10]. The N501Y, K417N, and E484K mutations in Beta variant may induce a conformational change of the spike protein and promote the infectivity of SARS-CoV-2 [11]. In addition, Beta variant is resistant to many monoclonal antibodies against the N-terminal domain and the RBD, mostly due to the E484K mutation [7,8,10]. Moreover, Delta variant had already spread to more 100 countries. L452R and T478K mutations of Delta variant could result in the reduction of antibody neutralization and induce a strong immune escape ability [12–14]. These mutations present new challenges for current therapies and vaccines.

In our previous studies, we have found that GB-1, developed from Chiehyuan herbal formula which obtained from Tian Shang Sheng Mu of Chiayi Puzi Peitian Temple, can inhibit ACE2 mRNA expression and ACE2 and TMPRSS2 protein expression in different human cells and decrease both ACE2 and TMPRSS2 expression levels of lung and kidney tissue in an animal model [15]. However, the effect of GB-1 on the binding of ACE2 and spike proteins of SARS-CoV-2 remains unclear. In this study, we investigated the effects of GB-1 on the interaction between ACE2 and SARS-CoV-2 spike protein.

2. Methods and materials

2.1. Preparation and quality control of GB-1

The GB-1 formula was developed from Chiehyuan herbal formula which obtained from Tian Shang Sheng Mu of Chiayi Puzi Peitian Temple in Taiwan. Briefly, 25 g of *Glycyrrhiza uralensis* Fisch. ex DC. (Fig. 1A, originated from Hangjinqi, Inner Mongolia, voucher reference: No 0.7 H-E014) and 5 g of *Camellia sinensis* var. assamica (Fig. 1B, originated from Chiayi city, Taiwan, voucher reference: No 0.7 H-Y059) were weighed. All herbs were authenticated by pharmacist in the Chinese pharmacy department of Chiayi Chang Gung Memorial Hospital. Then, GB-1 (30 g) was soaked in 2000 mL water and boiling hot water for 25 min in thermal flasks, respectively. The water extracts (1500 mL) were filtered with filter paper to remove particulate matter. Then, the water extracts (1500 mL) were evaporated through reducing pressure to obtain viscous masses of 4 g for GB-1. These samples were stored at − 80 °C. For all experiments, final concentrations of the tested compound were prepared by diluting the stock with water.

Quality control of GB-1 was performed using High-performance Liquid Chromatography (HPLC) through the Agilent 1100 HPLC system. For (+)-catechin (from Sigma-Aldrich, Batch Number: BCCC3128), Column: C18(4.6 mm x 150 mm, 5 uM, Discovery®), mobile phase A: 0.3% phosphoric acid, mobile phase B: 100% acetonitrile (mobile phase: 0 min, 90:10; 16.2 min, 80:20; 23.4 min, 40:60; 23.76 min, 90:10), Flow rate: 0.7 mL/min, wavelength: 278 nm, Column temp: 30 ℃. For glycyrrhizic acid (from ChromaDex, Irvine, CA, USA), Column: C18 (4.6 mm x150mm,5uM, Discovery®). The mobile phase used for detection was 100% acetonitrile and 2% acetic acid at a ratio of 36% and 64%, respectively. Flow rate: 0.6 mL/min, wavelength: 278 nm, Column temp: 25 ℃.

2.2. Cell culture and treatment

293 T cells (human embryonic kidney cell line) were obtained from the Bioresource Collection and Research Center, Taiwan. 293 T cells were cultured in Dulbecco's Modified Eagle's medium (DMEM, Invitrogen Corp., Carlsbad, CA), supplemented with 10% FBS at 37 ℃ and 5% CO2. The pCEP4-myc-ACE2 plasmid was a gift from Erik Procko (Addgene plasmid # 141185; http://n2t.net/addgene:141185; RRID: Addgene_141185). pcDNA3-SARS-CoV-2-S-RBD-sfGFP plasmid was a gift from Erik Procko (Addgene plasmid # 141184; http://n2t.net/addgene:141184; RRID:Addgene_141184). Before treatment, 293 T cells were cultured to 60–70% confluence. Then, cultured medium was replaced with fresh medium containing indicated compounds in water at the indicated concentrations. 293 T cells treated with water were used as controls. 293 T cells without treatment were used as blank control.

2.3. 2,3-bis-(2-methoxy-4-nitro-5-sulfophenyl)− 2 H-tetrazolium-5-carboxanilide assay (XTT assay)

293 T cell lines were cultured at a density of 1×10^3 per well of 96-well plates, in DMEM with 10% FBS. Once attached, the cultured medium was replaced with fresh medium with 10% FBS. 293 T cell were then treated with indicated drugs for indicated hours; and absorbance were measured using the XTT assay kit (Roche, catalog number: 11465015001) depending on the manufacturer's instructions. The XTT formazan complex was quantitatively measured at 492 nm using an ELISA reader (Bio-Rad Laboratories, Inc.).

2.4. ACE2/SARS-CoV-2 spike inhibitor screening assay

The ACE2/SARS-CoV-2 spike inhibitor screening assay were performed as described previously [16] using the ACE2: SARS-CoV-2 spike inhibitor screening assay kit (BPS Bioscience Cat. number #79936) according to the manufacturer's instructions. Briefly, ACE2 solution was used to coat a 96-well nickel-coated plate and washing the plate. Then, the plate was incubated with a blocking buffer. Next, the indicated compounds were added and incubated for 1 h at room temperature with slow shaking. After the incubation, SARS-CoV-2 Spike (RBD)-Fc was added to each well, except to the blank and incubated the reaction with slow shaking. After incubation with a blocking buffer, an anti-mouse-Fc-HRP and incubate and an HRP substrate was added to the plate to produce chemiluminescence, which then can be measured using microplate reader.

2.5. Flow cytometry analysis of ACE2-Spike protein binding

The flow cytometry analysis of ACE2-S Binding were performed as described previously [17]. Briefly, 293 T cells were transfected with pCEP4-MYC-ACE2 or pcDNA3-SARS-CoV-2-S-RBD-sfGFP plasmids (500 ng DNA per mL of culture at 2×10^6 / mL) using lipofectamine 2000 (ThermoFisher). The medium with indicated RBD-sfGFP were collected from 293 T cells which transfected with pcDNA3-SARS-CoV-2-S-RBD-sfGFP plasmid after 48 h. After pretreated by indicated drugs for 24 h, 293 T cells which transfected with pCEP4-MYC-ACE2 plasmid were washed with ice-cold PBS-BSA, and incubated for 30 min on ice with medium containing RBD-sfGFP and the anti-MYC Alexa 647 (clone 9B11, Cell Signaling Technology). Then, cells were washed twice with PBS-BSA and analyzed by the flow cytometer BD FACSCanto (Becton Dickinson).

2.6. Site-directed mutagenesis

The QuikChange Lightning Site-Directed Mutagenesis Kit (Agilent Technologies Inc., Santa Clara, CA) was used to introduce amino acid substitutions (N501Y, E484K, K417N, K417N-E484K-N501Y, K417T-E484K-N501Y or L452R-T478K) in pcDNA3-SARS-CoV-2-S-RBD-sfGFP plasmid by following the manufacturer's instructions.

2.7. Statistical analyses

All values were the means ± standard error of mean (SEM) of the replicate samples (n = 3–6, depending on the experiment). These experiments were repeated by a minimum of three times. Differences

between two groups were assessed using the unpaired two-tailed Student's *t*-test or by ANOVA if more than two groups were analyzed. For testing the significance of pairwise group comparisons, the Tukey test was used as a post-hoc test in ANOVA. For all comparisons, *P* values of < 0.05 were considered statistically significant. SPSS version 13.0 (SPSS Inc., Chicago, IL, USA) was used for all calculations.

3. Results

3.1. Identification of reference compounds in GB-1 by HPLC analysis

Glycyrrhizic acid (Fig. 1C) and (+)-Catechin (Fig. 1D) were used as the reference standards to validate the main compounds in GB-1. Glycyrrhizic acid (Fig. 1E) in *Glycyrrhiza uralensis* Fisch. ex DC. and (+)-catechin (Fig. 1F) in *Camellia sinensis* var. assamica were identified as the reference compounds in GB-1 through HPLC analysis.

3.2. Effect of GB-1 on cell variability of the 293 T cell line and the interaction between ACE2 and RBD with Wuhan type

Much previous research has used 293 T cells as a model to investigate the effect and mechanism of SARS-CoV-2 entry [17–19]. We used 293 T cells as a model to study the effect of GB-1 on the interaction between ACE2 and SARS-CoV-2 spike proteins. First, we used a XTT assay to investigate the cytotoxicity of GB-1–293 T cells. Our results showed that GB-1 treatment with concentrations of 100–300 μg/mL did not inhibit the variability of the 293 T cells after 24–48 h (Fig. 2A). These data suggest that 100–300 μg/mL GB-1 does not have significant cytotoxicity against the cell variability of the 293 T cell line. Next, we used a spike/ACE2 inhibitor screening assay kit to investigate the effect of GB-1 on the interaction between ACE2 and the spike protein of Wuhan-type SARS-CoV-2 [16]. As illustrated in Fig. 2B, we found that the binding of the Wuhan-type RBD of the spike protein to the ACE2 receptor was blocked by GB-1 in a concentration-dependent manner over the concentration range from 100 to 300 μg/mL (Fig. 2B).

3.3. Effect of GB-1 on the binding between ACE2 and RBD with K417N-E484K-N501Y mutation

Studies have reported that mutations (K417N, E484K and N501Y) in the RBD in SARS-CoV-2 are associated with higher infectivity and resistance to neutralization of several antibodies [11,20]. Next, we investigated the effect of GB-1 on the binding between ACE2 and RBD with K417N-E484K-N501Y mutation through dual-color flow cytometric analysis. For the dual-color flow cytometric analysis, 293 T cells expressing MYC-tagged ACE2 were incubated with medium containing the RBD of SARS-CoV-2 fused to superfolder green fluorescent protein [21]. After treatment of the cells with the indicated drugs, populations of cells that expressed MYC-tagged ACE2 at the cell surface with high or low binding to RBD were collected through fluorescence-activated cell sorting [17]. After treatment of the cells with the indicated concentration of GB-1, the number of 293 T cells with low binding to the RBD with K417N-E484K-N501Y mutation was significantly increased in both ACE2-positive cells and the top population in the 200–300 μg/mL GB-1 treatment group (Fig. 3A, B). The number of 293 T cells with high binding to the RBD with K417N-E484K-N501Y mutation was also decreased in ACE2-positive cells and the top population in the 200–300 μg/mL GB-1 treatment group (Fig. 3A, B). These results suggested that 200–300 μg/mL GB-1 blocked the binding between ACE2 and RBD with K417N-E484K-N501Y mutation.

3.4. Effect of GB-1 on the binding between ACE2 and RBD with K417T-E484K-N501Y mutation

Gamma variant could induce higher virus levels than earlier variants and have higher mortality [22]. The RBD in gamma variant contain

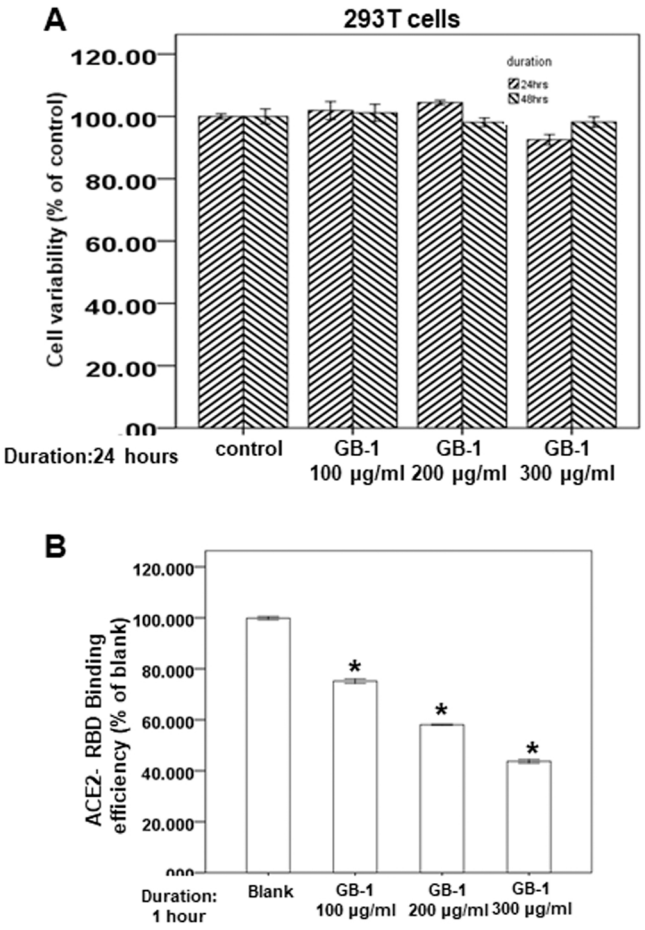

Fig. 2. Effect of GB-1 on cell variability of the 293 T cell line and the interaction between ACE2 and RBD with Wuhan type. (A) 293 T cells were measured by XTT assay after indicated hours of culturing in the presence of GB-1. (B) The indicated compounds were tested to evaluate their ability to inhibit the binding of spike protein to immobilized ACE2 by the ACE2/SARS-CoV-2 spike inhibitor screening assay. All the results are representative of at least three independent experiments. (Error bars=mean±S.E.M. Asterisks (*) mark samples significantly different from control group with $p < 0.05$).

N501Y, E484K and K417T mutations [22,23]. Next, we investigated the effect of GB-1 on the binding between ACE2 and RBD with K417T-E484K-N501Y mutation through dual-color flow cytometric analysis. After treatment of the cells with the indicated concentration of GB-1, the number of 293 T cells with high binding to the RBD with K417T-E484K-N501Y mutation was decreased in both ACE2-positive cells and the top population in the 200–300 μg/mL GB-1 treatment group (Fig. 4A, B). The number of 293 T cells with low binding to the RBD with K417T-E484K-N501Y mutation was decreased in ACE2-positive cells and the top population in the 200 μg/mL GB-1 treatment group (Fig. 4A, B). These results suggested that GB-1 can partially affect the binding between ACE2 and RBD with K417T-E484K-N501Y mutation.

3.5. Effect of GB-1 on the interaction between ACE2 and RBD with N501Y mutation

N501 is the important residue in the RBD of SARS-CoV-2 spike protein that is involved in critical contact with the interface of ACE2 [2,24]. Previous reports have demonstrated that RBD with N501Y mutation promoted binding to the ACE2 receptor more than did the Wuhan type and increased the infectivity of SARS-CoV-2 [24–29]. In our previous results, GB-1 could inhibit the binding between ACE2 and RBD with

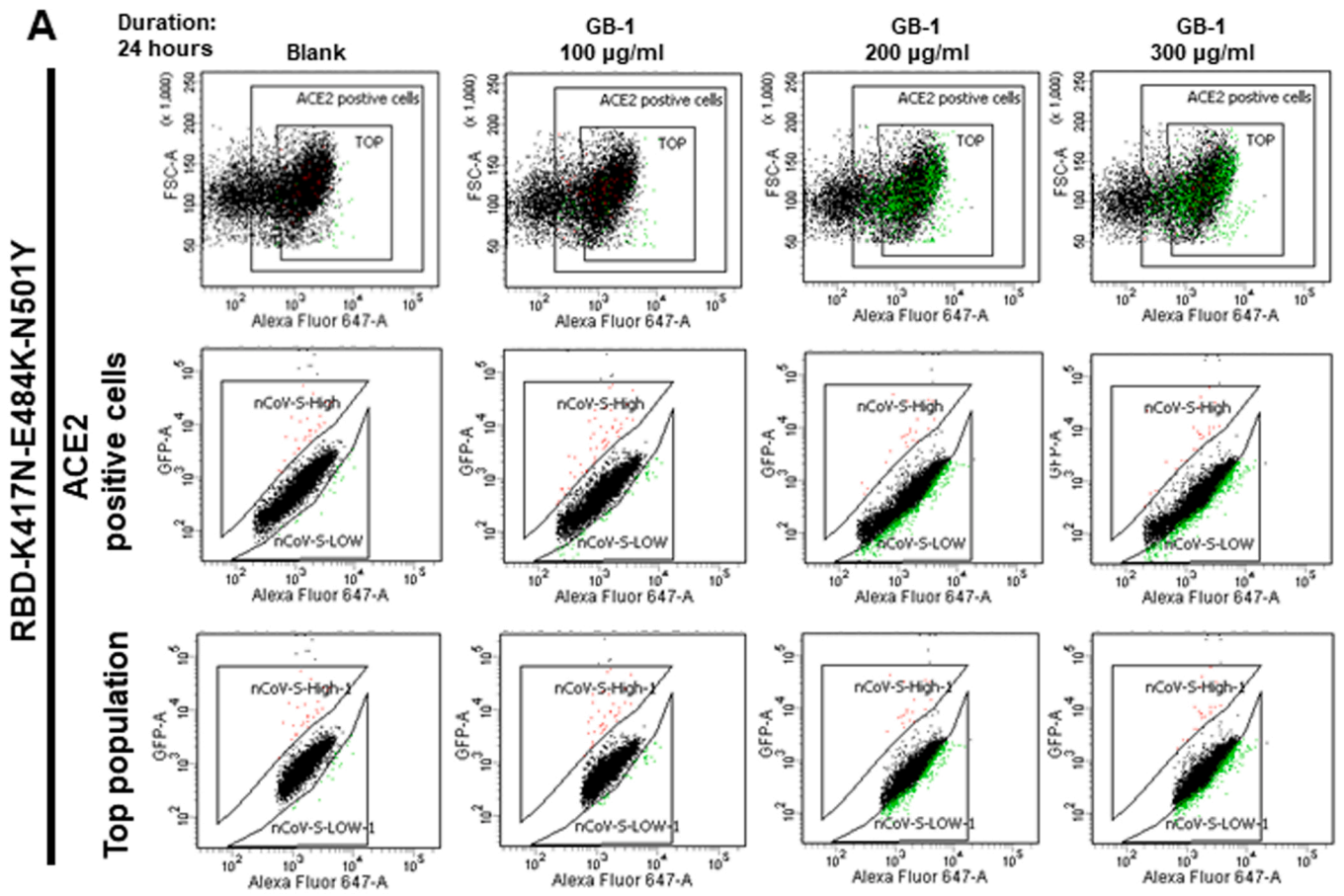

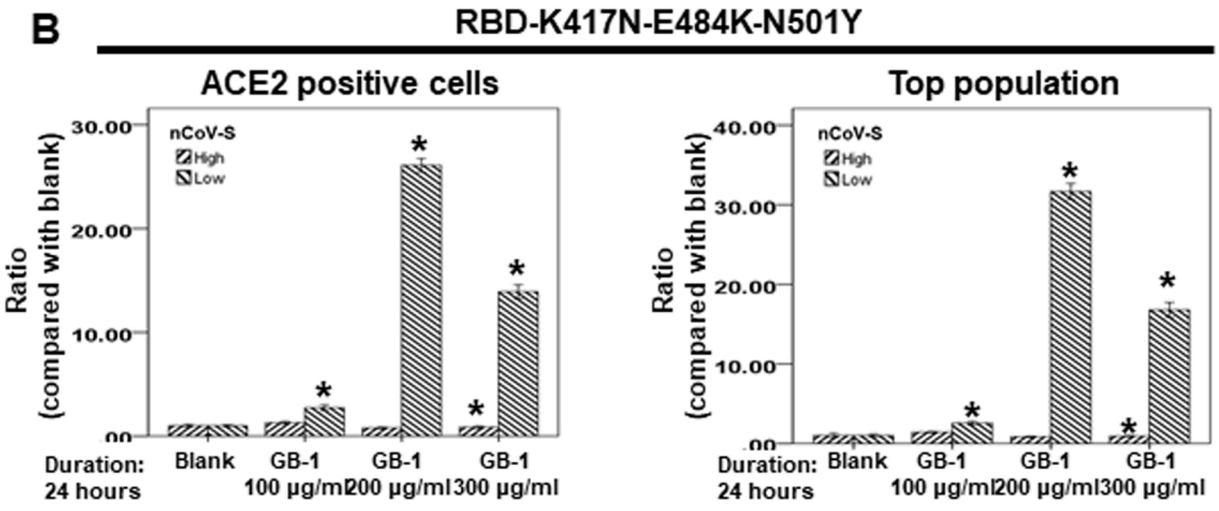

Fig. 3. Effect of GB-1 on interaction between ACE2 and RBD with K417N-E484K-N501Y mutation. (A) Flow cytometry analysis of ACE2-Spike protein binding. 293 T cells with pCEP4-MYC-ACE2 plasmid were incubated with RBD (K417N-E484K-N501Y)-sfGFP-containing medium and co-stained with fluorescent anti-MYC Alexa 647 to detect surface ACE2 by flow cytometry. During analysis, the top population were chosen from the ACE2-positive population. Then, two subsets of the ACE2-positive population were collected: the top population (nCoV-S-High sort, red gate) and the bottom population (nCoV-S-Low sort, green gate) based on the fluorescence of bound RBD(K417N-E484K-N501Y)-sfGFP relative to ACE2 surface expression. (B) Quantitative results of nCoV-S-High sort and nCoV-S-low sort, which were presented as ratio compared with blank, in the top population or ACE2-positive population. All the results are representative of at least three independent experiments. (Error bars = mean±S.E.M. Asterisks (*) mark samples significantly different from control group with $p < 0.05$).

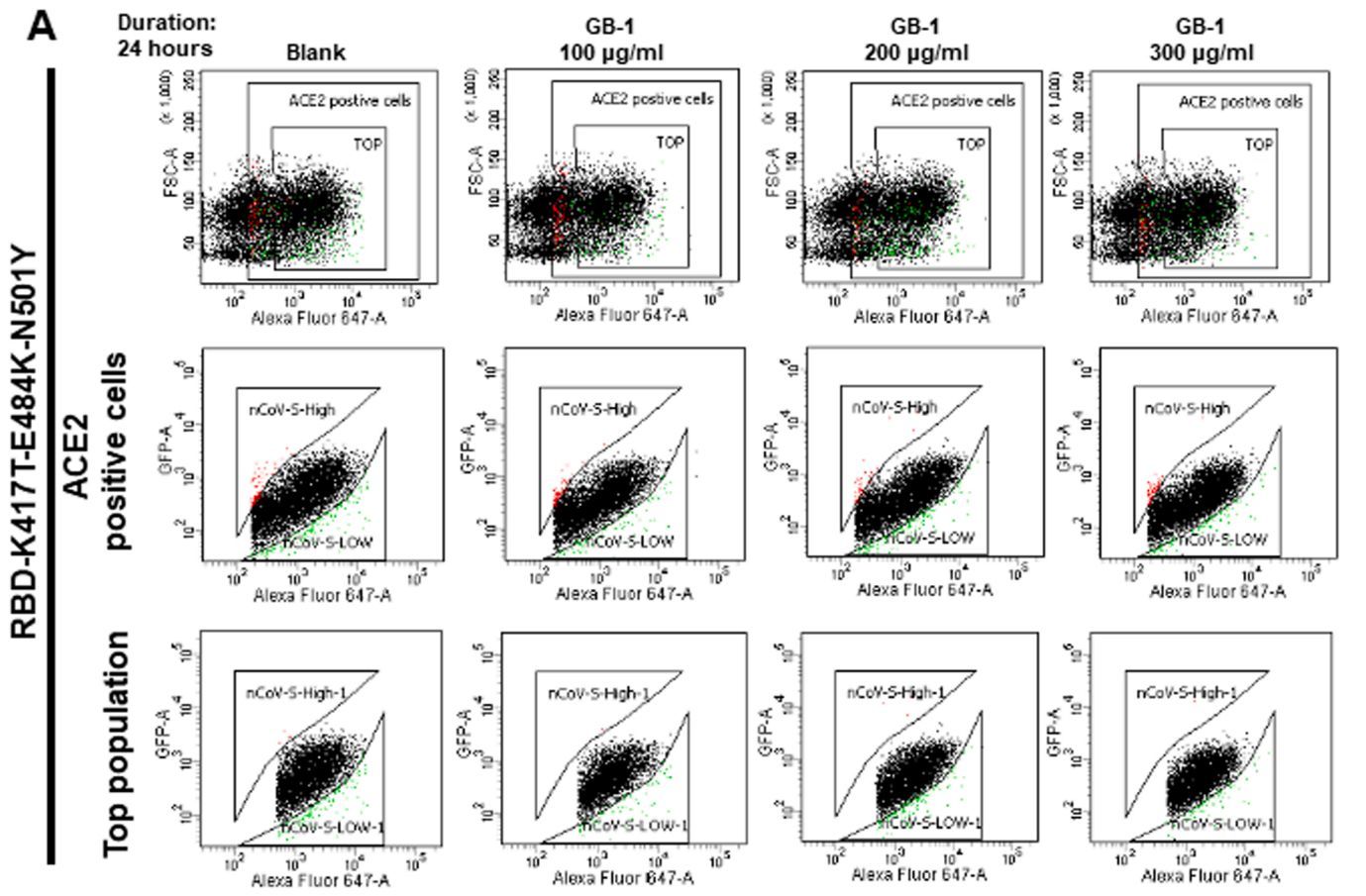

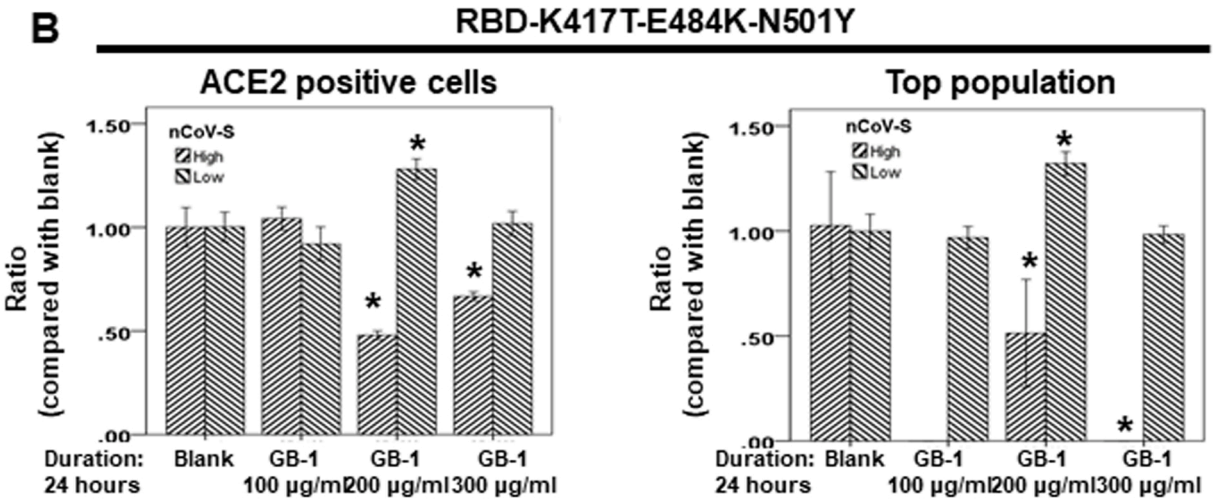

Fig. 4. Effect of GB-1 on interaction between ACE2 and RBD with K417T-E484K-N501Y mutation. (A) Flow cytometry analysis of ACE2-Spike protein binding. 293 T cells with pCEP4-MYC-ACE2 plasmid were incubated with RBD (K417T-E484K-N501Y)-sfGFP-containing medium and co-stained with fluorescent anti-MYC Alexa 647 to detect surface ACE2 by flow cytometry. During analysis, the top population were chosen from the ACE2-positive population. Then, two subsets of the ACE2-positive population were collected: the top population (nCoV-S-High sort, red gate) and the bottom population (nCoV-S-Low sort, green gate) based on the fluorescence of bound RBD(K417T-E484K-N501Y)-sfGFP relative to ACE2 surface expression. (B) Quantitative results of nCoV-S-High sort and nCoV-S-low sort, which were presented as ratio compared with blank, in the top population or ACE2-positive population. All the results are representative of at least three independent experiments. (Error bars=mean±S.E.M. Asterisks (*) mark samples significantly different from control group with $p < 0.05$).

K417N-E484K-N501Y mutation. Next, we investigated the effect of GB-1 on the interaction between ACE2 and RBD with N501Y mutation through dual-color flow cytometric analysis. After treatment of the cells with 100–300 μg/mL GB-1, the number of 293 T cells with low binding to the RBD with N501Y mutation was significantly increased in both ACE2-positive cells and the top population in a dose-dependent manner (Fig. 5A, B). The number of 293 T cells with high binding to the RBD with N501Y mutation was also decreased in both ACE2-positive cells and the top population in a dose-dependent manner (Fig. 5A, B). These results suggested that 100–300 μg/mL GB-1 inhibited the binding between ACE2 and RBD with N501Y mutation.

3.6. Effect of GB-1 on the interaction between ACE2 and RBD with E484K mutation

The previous studies showed that E484K mutation can completely abolish the binding of RBD to bamlanivimab [7,8]. Next, we investigated the effect of GB-1 on the interaction between ACE2 and RBD with E484K mutation through dual-color flow cytometric analysis. After treatment of the cells with the indicated concentration of GB-1, the number of 293 T cells with low binding to the RBD with E484K mutation was significantly increased in both ACE2-positive cells and the top population (Fig. 6A, B). The number of 293 T cells with high binding to the RBD with E484K mutation was also decreased in both ACE2-positive cells and the top population (Fig. 6A, B). These results suggested that 300 μg/mL GB-1 significantly inhibited the binding between ACE2 and RBD with E484K mutation.

3.7. Effect of GB-1 on the interaction between ACE2 and RBD with K417N mutation

K417 residue is located at the N-terminus of a short helix of the RBD and buried upon binding to ACE2 [30]. K417N usually co-occurs with E484K and N501Y in both Beta variant and Gamma variant [31]. K417N can block the hydrogen bond with ACE2-reducing affinity [30]. Despite the loss in the binding affinity between RBD and ACE2, the K417N mutation can escape neutralization by several monoclonal antibodies and decreases the efficiency of some vaccines [31]. For this reason, we investigated the effect of GB-1 on the interaction between ACE2 and RBD with K417N mutation of RBD through dual-color flow cytometric analysis. After treatment of the cells with the indicated concentration of GB-1, the number of 293 T cells with high binding to the RBD with K417N mutation was not increased in both ACE2-positive cells and the top population (Fig. 7A, B). The number of 293 T cells with low binding to the RBD with K417N mutation was decreased in both ACE2-positive cells and the top population (Fig. 7A, B). These results suggested that 100–300 μg/mL GB-1 cannot affect the binding between ACE2 and RBD with K417N mutation.

3.8. Effect of GB-1 on the binding between ACE2 and RBD with L452R-T478K mutation

In early 2021, delta variant (B.1.617.2) is discovered in India and has demonstrated increased transmissibility [23]. L452R and T478K mutations of RBD in delta variant could induce a strong immune escape ability [12–14]. Next, we investigated the effect of GB-1 on the binding between ACE2 and RBD with L452R-T478K mutation through dual-color flow cytometric analysis. After treatment of the cells with GB-1, the number of 293 T cells with high binding to the RBD with L452R-T478K mutation was significantly decreased in both ACE2-positive cells and the top population in GB-1 treatment group (Fig. 8A, B). The number of 293 T cells with low binding to the RBD with L452R-T478K mutation was also increased in ACE2-positive cells and the top population in the 200–300 μg/mL GB-1 treatment group (Fig. 8A, B). These results suggested that 200–300 μg/mL GB-1 blocked the binding between ACE2 and RBD with L452R-T478K mutation.

3.9. Effect of glycyrrhizic acid on the binding between ACE2 and RBD

The dry root of *Glycyrrhiza uralensis* (GU) (Fig. 1A) is the major component of GB-1 and is commonly used in Taiwan and worldwide for food and medicine. Glycyrrhizic acid (Fig. 1C) is the reference compound of *Glycyrrhiza uralensis* Our results indicated that GB-1 blocked the binding between ACE2 and RBD with Wuhan type or K417N-E484K-N501Y mutation (Figs. 2B and 3). Next, we investigated the effect of glycyrrhizic acid on the interaction between ACE2 and RBD with Wuhan type or K417N-E484K-N501Y mutation. After treatment of the cells with glycyrrhizic acid, the number of 293 T cells with low binding to the RBD with Wuhan type was significantly increased in both ACE2-positive cells and the top population in the 50 μg/mL glycyrrhizic acid treatment group (Fig. 9A, B). The number of 293 T cells with high binding to the RBD with Wuhan type was also decreased in ACE2-positive cells and the top population in the 50 μg/mL glycyrrhizic acid treatment group (Fig. 9A, B). However, the number of 293 T cells with high binding to the RBD with K417N-E484K-N501Y mutation was not increased in both ACE2-positive cells and the top population after 50 μg/mL glycyrrhizic acid treatment (Fig. 10A, B). The number of 293 T cells with low binding to the RBD with K417N-E484K-N501Y mutation was not affected in both ACE2-positive cells and the top population after 50 μg/mL glycyrrhizic acid treatment (Fig. 10A, B). These results suggested that 50 μg/mL glycyrrhizic acid blocked the binding between ACE2 and RBD with Wuhan type. However, 50 μg/mL glycyrrhizic acid cannot affect the binding between ACE2 and RBD with K417N-E484K-N501Y mutation.

4. Discussion

SARS-CoV-2 Beta variant was first isolated in October 2020 in Nelson Mandela Bay, South Africa [31]. Beta variant contains nine mutations in SARS-CoV-2 spike protein: D614G, Δ242–Δ244, R246I, K417N, E484K, N501Y, and A701V [10]. The previous studies reported that K417N involves in the interaction between spike protein and ACE2 [7,8]. Although E484 is located outside of ACE2 binding area, E484K mutation can abolish the binding of RBD to some antibodies, including bamlanivimab[7,8]. The first characterization report from Haolin Liu and colleagues showed that N501Y mutation increases the binding affinity between spike protein and ACE2 [25,26]. Moreover, K417N-E484K-N501Y mutations within RBD of the virus could increase higher binding affinity to ACE2 than the wildtype RBD [7,8]. In our results, GB-1 has higher inhibitory ability in the variant with K417N-E484K-N501Y mutation than the variant with K417T-E484K-N501Y mutation. Moreover, GB-1 inhibited the binding between ACE2 and RBD with N501Y mutation or E484K mutation, but not K417N mutation. The previous study reported that desolvation energy, restraints violation energy, Van der Waals energy, electrostatic energy, and buried surface area are different between K417N-E484K-N501Y mutation and K417T-E484K-N501Y mutation [32]. These results suggest that the interaction between ACE2 and E484 or N501 of RBD may be the major target of GB-1. The different K417N/T mutations could affect the inhibitory ability of GB-1 on the binding between ACE2 and RBD with K417N-E484K-N501Y mutation or K417T-E484K-N501Y mutation. However, the deeper mechanism of GB-1 on these SARS-CoV-2 mutations is still unclear. Thus, further investigation is necessary.

The antiviral effects of glycyrrhyza glabra were first reported by the study of Pompei and collaborators [33]. Moreover, several studies discovered the anti-viral effect of glycyrrhizin or licorice extracts on herpes simplex virus type 1, Epstein-Barr, pseudorabies, paramixoviriade Newcastle or human respiratory syncytial viruses, rhabdoviridae vesicular stomatitis virus and varicella-zoster viruses [33–36]. For SARS-CoV-2, a recent study showed that glycyrrhizic acid has the highest affinity toward the viral main protease (Mpro), representing binding energy through molecular docking simulation studies [37,38]. An in vitro study also showed that glycyrrhizic acid has inhibitory ability

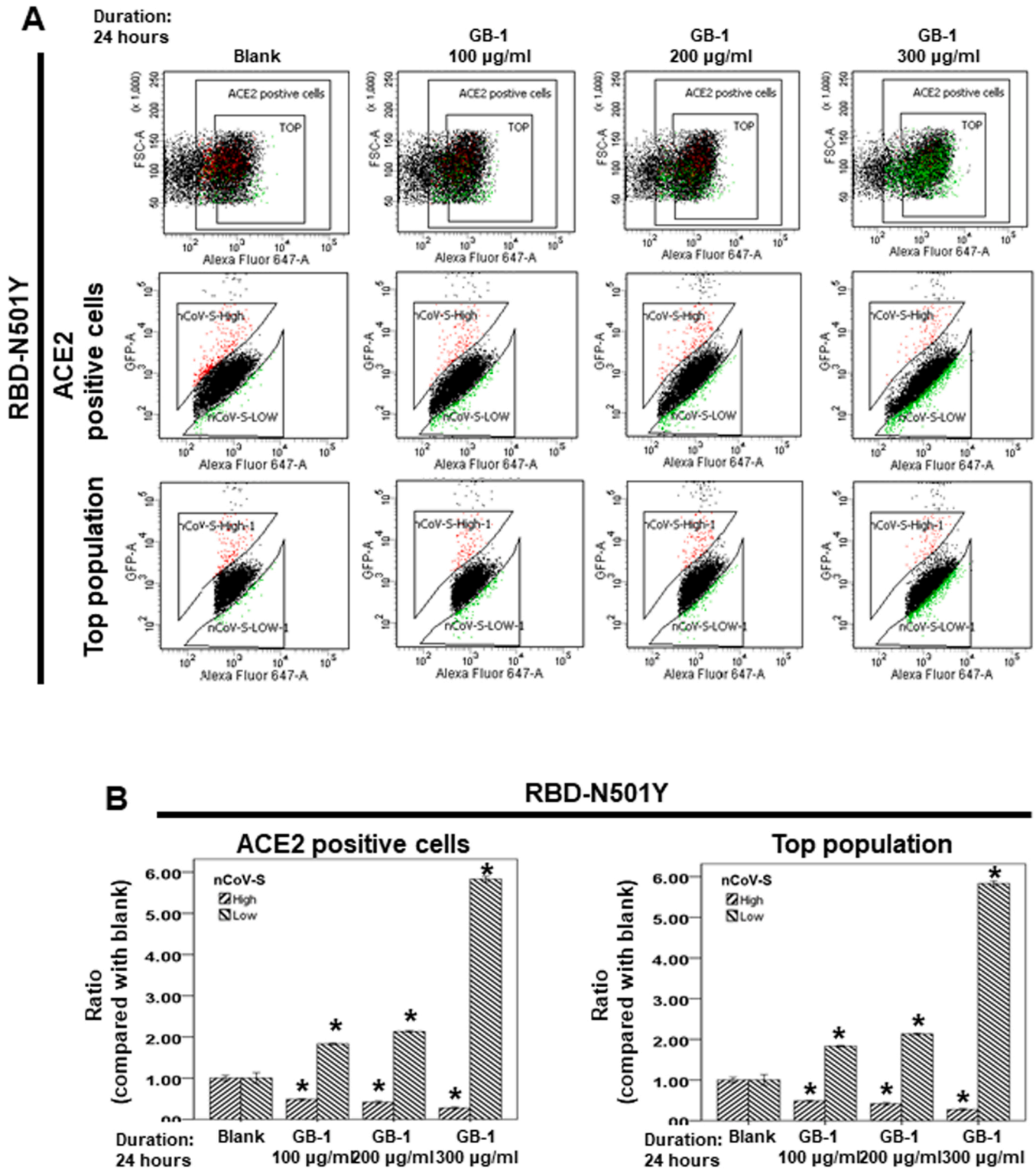

Fig. 5. Effect of GB-1 on interaction between ACE2 and RBD with N501Y mutation. Flow cytometry analysis of ACE2-Spike protein binding. (A) 293 T cells with pCEP4-myc-ACE2 plasmid were incubated with RBD (N501Y)-sfGFP-containing medium and co-stained with fluorescent anti-MYC Alexa 647 to detect surface ACE2 by flow cytometry. During analysis, the top population were chosen from the ACE2-positive population. Then, two subsets of the ACE2-positive population were collected: the top population (nCoV-S-High sort, red gate) and the bottom population (nCoV-S-Low sort, green gate) based on the fluorescence of bound RBD (N501Y)-sfGFP relative to ACE2 surface expression. (B) Quantitative results of nCoV-S-High sort and nCoV-S-low sort, which were presented as ratio compared with blank, in the top population or ACE2-positive population. All the results are representative of at least three independent experiments. (Error bars=mean±S.E.M. Asterisks (*) mark samples significantly different from control group with $p < 0.05$).

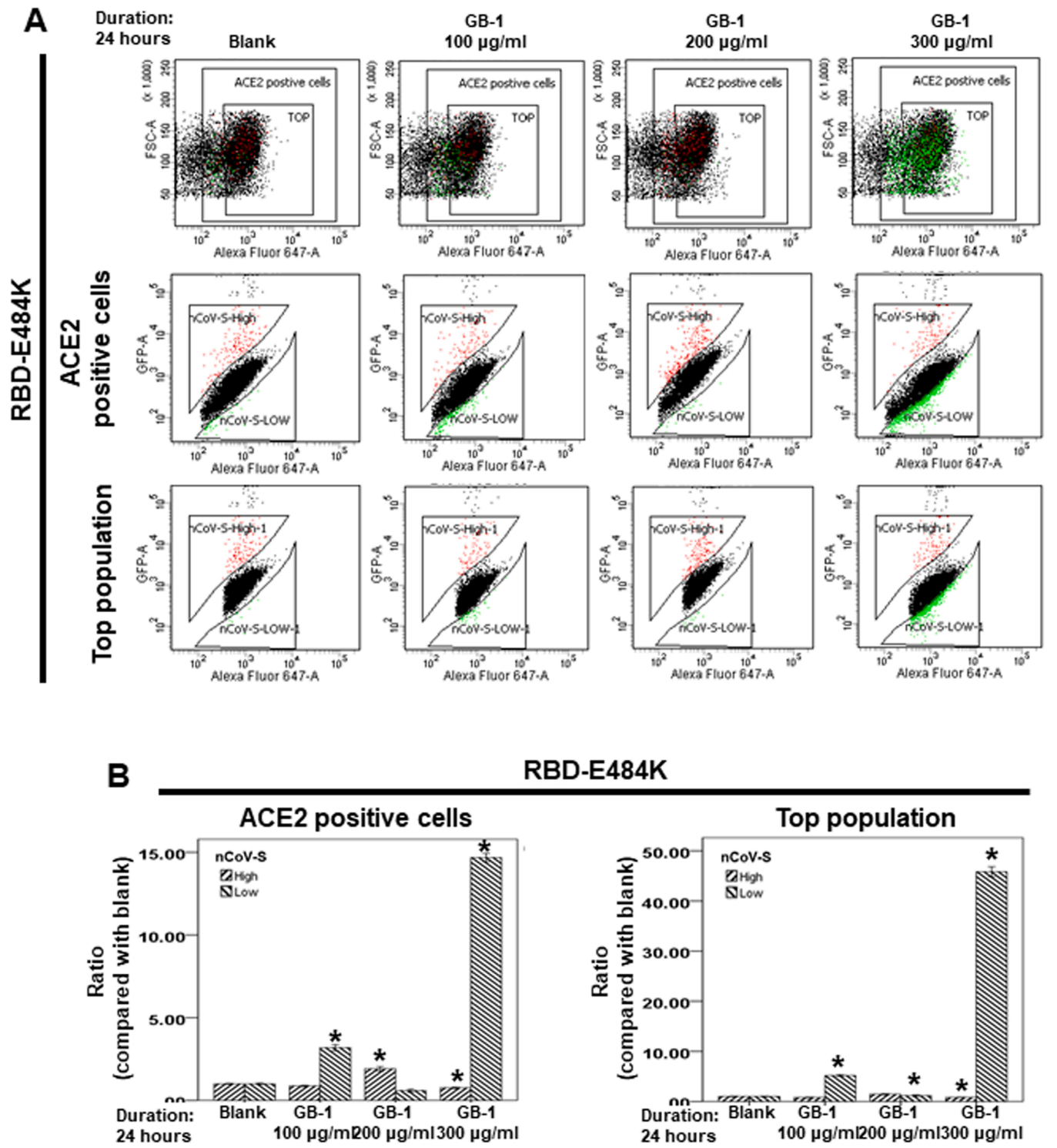

Fig. 6. Effect of GB-1 on interaction between ACE2 and RBD with E484K mutation. Flow cytometry analysis of ACE2-Spike protein binding. (A) 293 T cells with pCEP4-myc-ACE2 plasmid were incubated with RBD (E484K)-sfGFP-containing medium and co-stained with fluorescent anti-MYC Alexa 647 to detect surface ACE2 by flow cytometry. During analysis, the top population were chosen from the ACE2-positive population. Then, two subsets of the ACE2-positive population were collected: the top population (nCoV-S-High sort, red gate) and the bottom population (nCoV-S-Low sort, green gate) based on the fluorescence of bound RBD (E484K)-sfGFP relative to ACE2 surface expression. (B) Quantitative results of nCoV-S-High sort and nCoV-S-low sort, which were presented as ratio compared with blank, in the top population or ACE2-positive population. All the results are representative of at least three independent experiments. (Error bars=mean±S.E.M. Asterisks (*) mark samples significantly different from control group with $p < 0.05$).

for SARS-CoV-2 replication through blocking Mpro [39]. In another molecular docking study, an ephedra–glycyrrhiza pairing could bind well to Mpro, SARS-CoV-2 spike protein (Wuhan type), and ACE2 [40]. Moreover, a pharmacoinformatics study indicated that glycyrrhizic acid is suited to the binding pocket of SARS-CoV-2 spike glycoprotein (Wuhan type; Protein Data Bank identifier 6VSB) and prohibits the entry of SARS-CoV-2 into the host cell, as determined through a molecular docking simulation with AutoDock Vina software [41]. Jingjing Li and

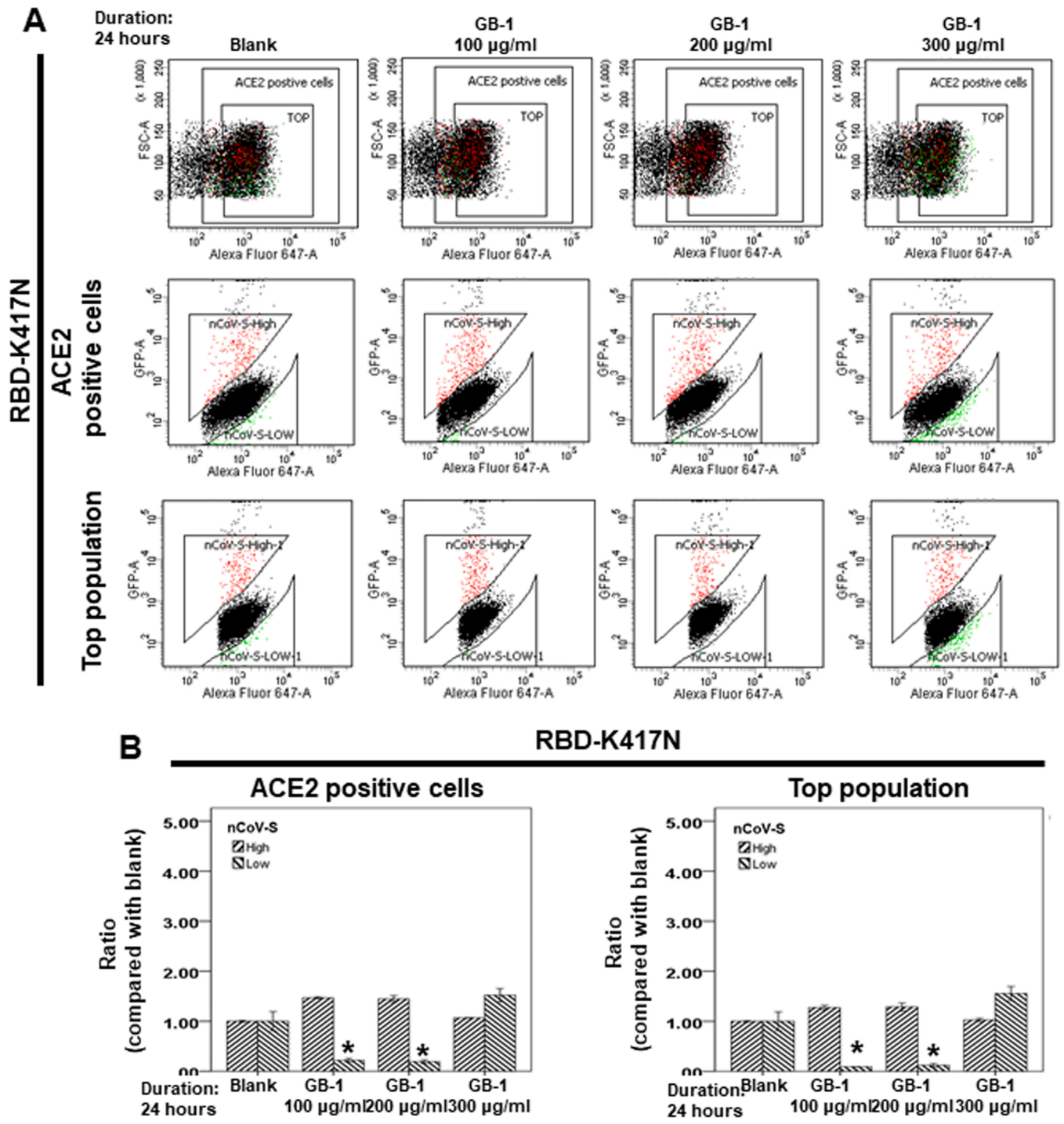

Fig. 7. Effect of GB-1 on interaction between ACE2 and RBD with K417N. Flow cytometry analysis of ACE2-Spike protein binding. (A) 293 T cells with pCEP4-myc-ACE2 plasmid were incubated with RBD (K417N)-sfGFP-containing medium and co-stained with fluorescent anti-MYC Alexa 647 to detect surface ACE2 by flow cytometry. During analysis, the top population were chosen from the ACE2-positive population. Then, two subsets of the ACE2-positive population were collected: the top population (nCoV-S-High sort, red gate) and the bottom population (nCoV-S-Low sort, green gate) based on the fluorescence of bound RBD (K417N)-sfGFP relative to ACE2 surface expression. (B) Quantitative results of nCoV-S-High sort and nCoV-S-low sort, which were presented as ratio compared with blank, in the top population or ACE2-positive population. All the results are representative of at least three independent experiments. (Error bars=mean±S.E.M. Asterisks (*) mark samples significantly different from control group with $p < 0.05$).

colleagues reported that glycyrrhizic acid can inhibit SARS-CoV-2 lentivirus infection through blocking the interaction between spike protein-host cells[42]. Zhaoyan Zhao and colleagues reported that glycyrrhizic acid nanoparticles can inhibit the proliferation of the murine coronavirus MHV-A59[43]. Glycyrrhizin nicotinate derivatives also can block SARS-CoV-2 virus and HIV-1 pseudoviruses infection[44]. However, the effect of glycyrrhizic acid on the binding between ACE2 and SARS-CoV-2 spike protein with mutations is unclear. In our results, we discovered that glycyrrhizic acid could block the binding between ACE2 and the Wuhan-type RBD through dual-color flow cytometric analysis. This result is consistent with a previous in silico study [41]. The results suggested that glycyrrhizic acid could decrease the viral

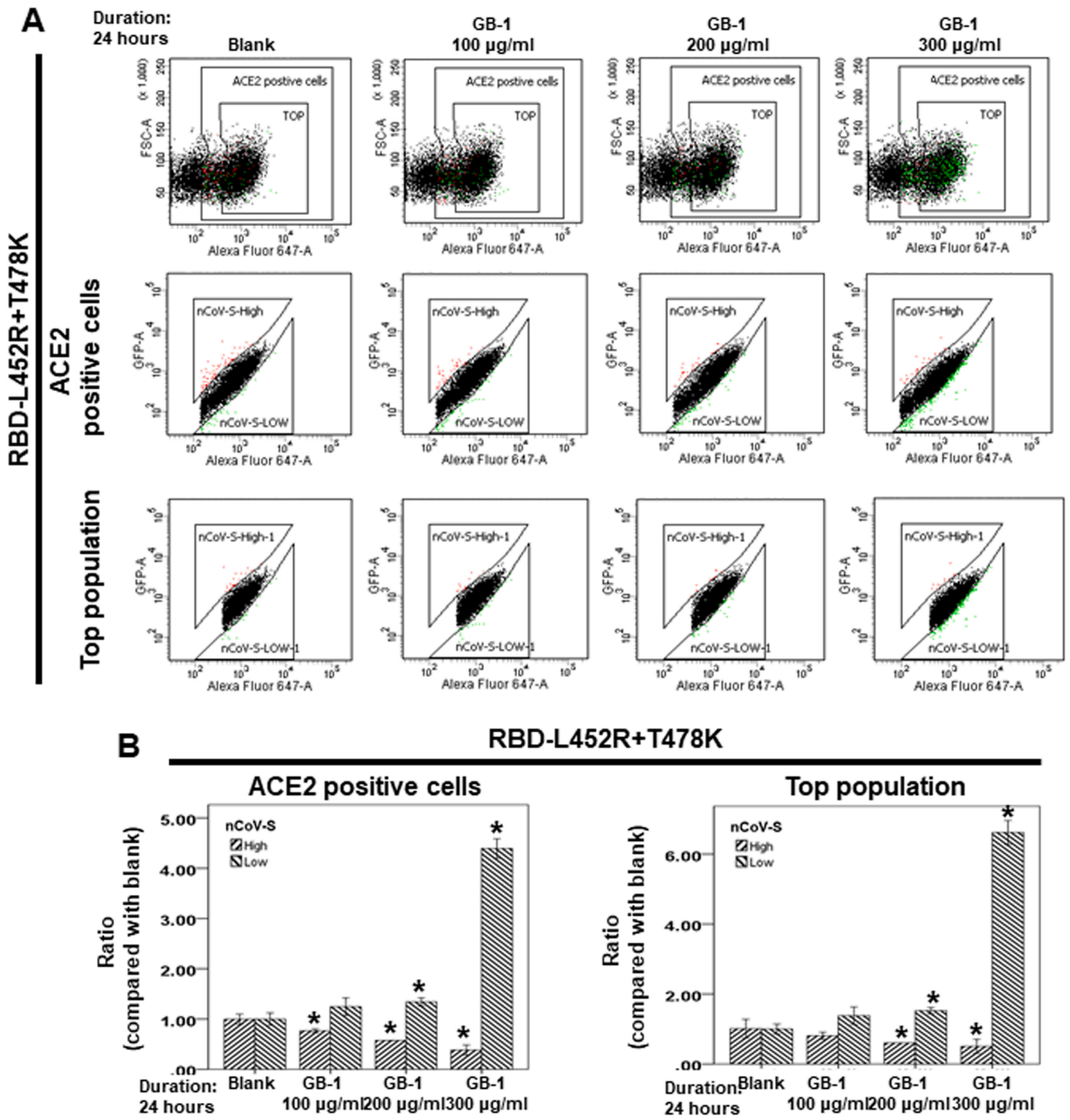

Fig. 8. Effect of GB-1 on interaction between ACE2 and RBD with L452R-T478K mutation. (A) Flow cytometry analysis of ACE2-Spike protein binding. 293 T cells with pCEP4-MYC-ACE2 plasmid were incubated with RBD (L452R-T478K)-sfGFP-containing medium and co-stained with fluorescent anti-MYC Alexa 647 to detect surface ACE2 by flow cytometry. During analysis, the top population were chosen from the ACE2-positive population. Then, two subsets of the ACE2-positive population were collected: the top population (nCoV-S-High sort, red gate) and the bottom population (nCoV-S-Low sort, green gate) based on the fluorescence of bound RBD(L452R-T478K)-sfGFP relative to ACE2 surface expression. (B) Quantitative results of nCoV-S-High sort and nCoV-S-low sort, which were presented as ratio compared with blank, in the top population or ACE2-positive population. All the results are representative of at least three independent experiments. (Error bars=mean±S.E.M. Asterisks (*) mark samples significantly different from control group with $p < 0.05$).

transmission rate of Wuhan-type SARS-CoV-2. However, 50 μg/mL glycyrrhizic acid did not affect the binding between ACE2 and RBD with K417N-E484K-N501Y mutation. The previous report showed that epigallocatechin gallate, theasinensin A and theaflavin 3,3′-di-O-gallate significantly inhibited interaction between recombinant ACE2 and RBD of spike protein [45]. It is possible that the other index compounds in black tea of GB-1 could block the binding between ACE2 and RBD with K417N-E484K-N501Y mutation, except glycyrrhizic acid.

In our previous study, we discovered that theaflavin, the other index compound of GB-1, has a potential chemical structure of anti-SARS-CoV-2 RNA-dependent RNA polymerase [46]. We also discovered that GB-1 could inhibit ACE2 and TMPRSS2 protein expression in different cell lines without cytotoxicity and lung and kidney tissue without nephrotoxicity and hepatotoxicity in animal model [15]. In this study, we

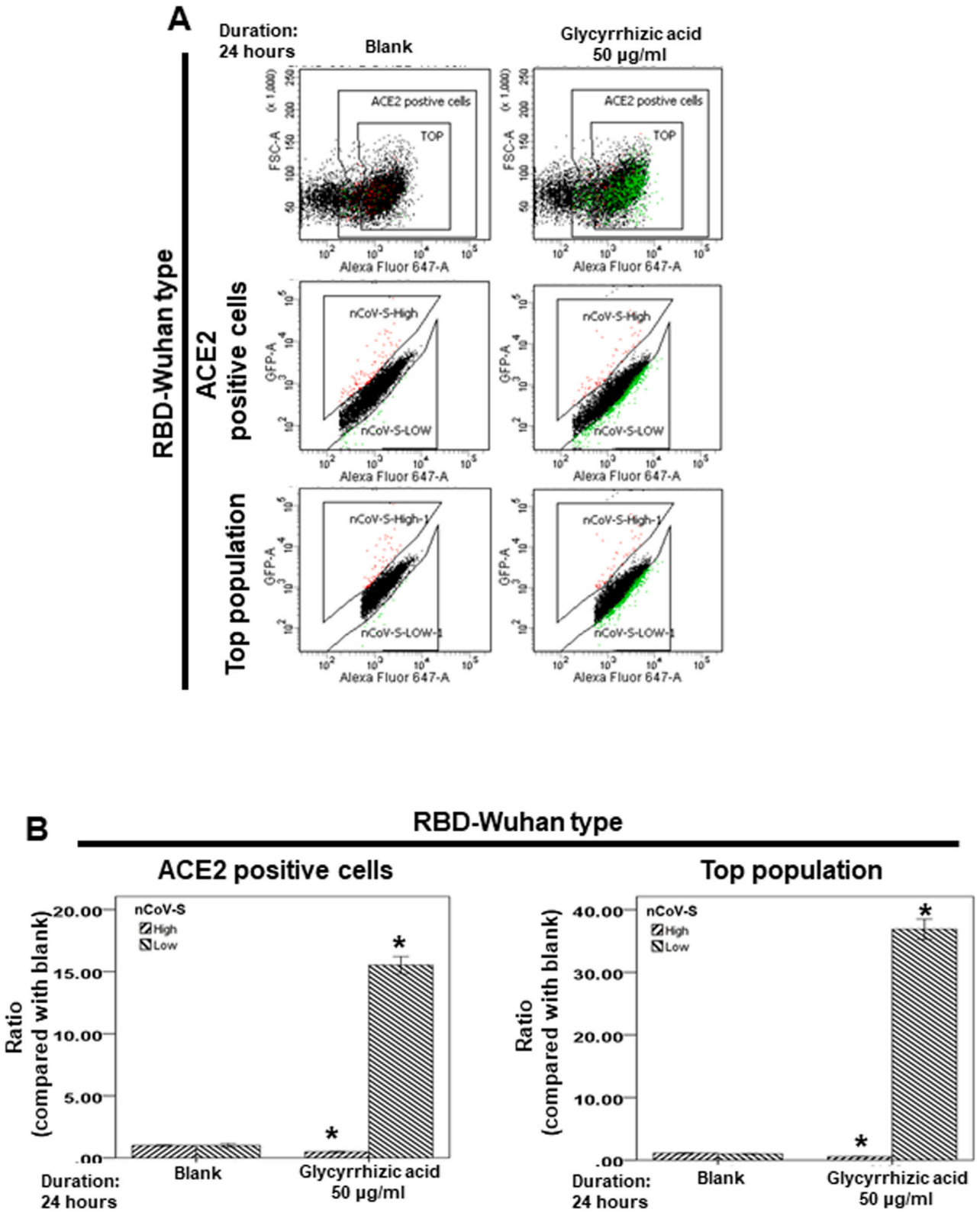

Fig. 9. Effect of glycyrrhizic acid on interaction between ACE2 and RBD with Wuhan type. (A) Flow cytometry analysis of ACE2-Spike protein binding. 293 T cells with pCEP4-MYC-ACE2 plasmid were incubated with RBD (Wuhan type)-sfGFP-containing medium and co-stained with fluorescent anti-MYC Alexa 647 to detect surface ACE2 by flow cytometry. During analysis, the top population were chosen from the ACE2-positive population. Then, two subsets of the ACE2-positive population were collected: the top population (nCoV-S-High sort, red gate) and the bottom population (nCoV-S-Low sort, green gate) based on the fluorescence of bound RBD (Wuhan type)-sfGFP relative to ACE2 surface expression. (B) Quantitative results of nCoV-S-High sort and nCoV-S-low sort, which were presented as ratio compared with blank, in the top population or ACE2-positive population. All the results are representative of at least three independent experiments. (Error bars=mean±S.E.M. Asterisks (*) mark samples significantly different from control group with $p < 0.05$).

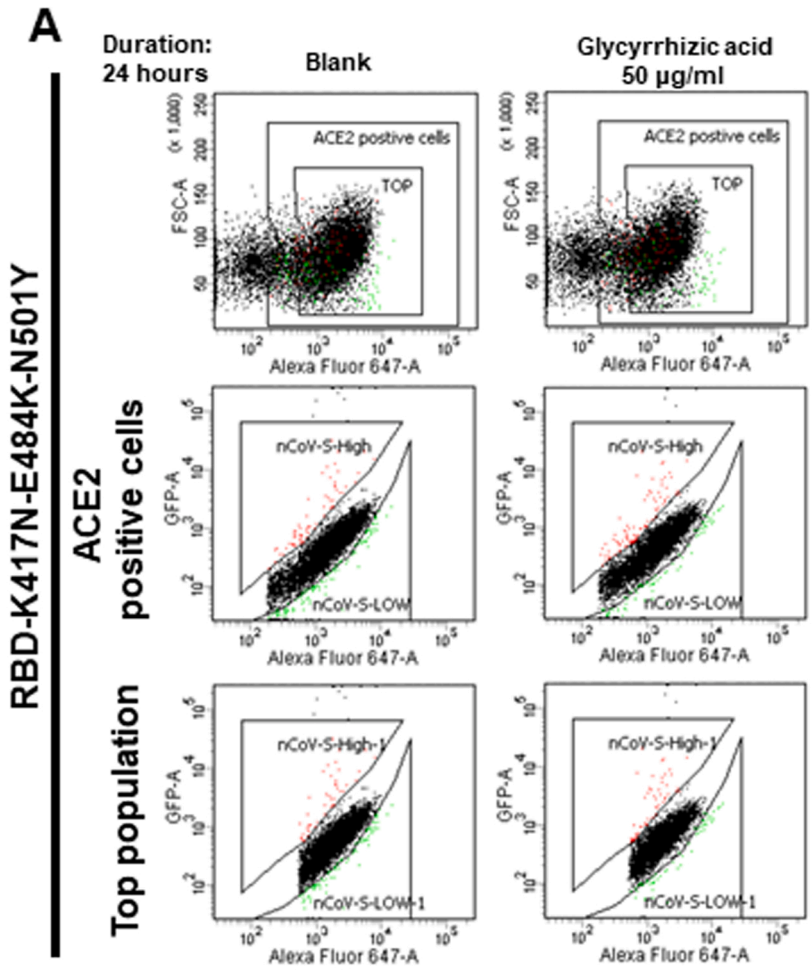

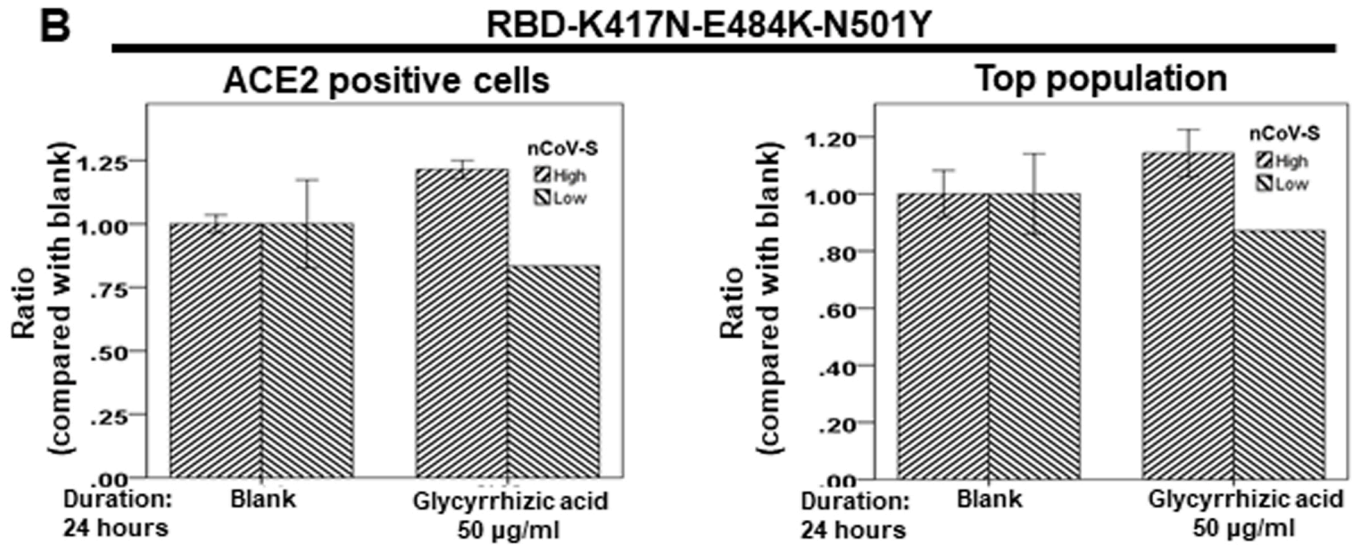

Fig. 10. Effect of glycyrrhizic acid on interaction between ACE2 and RBD with K417N-E484K-N501Y mutation. (A) Flow cytometry analysis of ACE2-Spike protein binding. 293 T cells with pCEP4-MYC-ACE2 plasmid were incubated with RBD (K417N-E484K-N501Y)-sfGFP-containing medium and co-stained with fluorescent anti-MYC Alexa 647 to detect surface ACE2 by flow cytometry. During analysis, the top population were chosen from the ACE2-positive population. Then, two subsets of the ACE2-positive population were collected: the top population (nCoV-S-High sort, red gate) and the bottom population (nCoV-S-Low sort, green gate) based on the fluorescence of bound RBD (K417N-E484K-N501Y)-sfGFP relative to ACE2 surface expression. (B) Quantitative results of nCoV-S-High sort and nCoV-S-low sort, which were presented as ratio compared with blank, in the top population or ACE2-positive population. All the results are representative of at least three independent experiments. (Error bars=mean±S.E.M. Asterisks (*) mark samples significantly different from control group with $p < 0.05$).

discovered that GB-1 blocked the binding between ACE2 and RBD with Wuhan-type or K417N-E484K-N501Y mutation. These results suggest that GB-1 may block the entry of SARS-CoV-2 into the host cell through several different mechanisms.

In conclusion, our results suggest that GB-1 could be a candidate for prophylaxis against some variants of SARS-CoV-2 infection through the inhibition of the binding between ACE2 and RBD with mutations (N501Y, E484K, L452R-T478K or K417N-E484K-N501Y). However, the exact clinical effect remains unknown. Thus, further clinical research is necessary to confirm the protective effects of GB-1 against SARS-CoV-2 infection.

Funding

Financial support was obtained from grant MOST 109-2320-B-182-021-MY3 from Ministry of Science and Technology (TW) and CORPG6K0211 from Chang Gung Memorial Hospital (Chiayi) to Dr. Ching Yuan Wu. The funding bodies allowed to the design of the study and collection, analysis, and interpretation of data and in writing the manuscript.

CRediT authorship contribution statement

Ching-Yuan Wu: Conceptualization, Methodology, Software. **Ming-Shao Tsai:** Data curation, Writing – original draft preparation. **Yu-Shih Lin:** Visualization, Investigation. **Li-Hsin Shu:** Visualization, Investigation. **Yu-Ching Cheng:** Visualization, Investigation. **Hung-Te Liu:** Visualization, Investigation. **Wei-Tai Shih:** Supervision, Revised the manuscript. **Cheng-Ming Hsu:** Supervision, Revised the manuscript. **Reming-Albert Yeh:** Supervision, Revised the manuscript. **Yao-Hsu Yang:** Software, Analyzed the data, Validation. **Geng-He Chang:** Software, Analyzed the data, Validation. Rou-Chen Shen. **Yu-Huei Wu:** Writing – review & editing. **Yu-Heng Wu:** Writing – review & editing.

Conflict of interest statement

The authors declare no conflict of interest.

Data Availability

Data will be made available on request. All data generated or analyzed during this study are indicated in this article (with no patient data). The datasets generated during and /or analyzed during the current study are available from the corresponding author on reasonable request.

Acknowledgements

The authors acknowledge the Health Information and Epidemiology Laboratory at the Chiayi Chang Gung Memorial Hospital for the comments and assistance in data analysis. The authors also thank the research assists by Chang Gung Medical Foundation and Ministry of Science and Technology, Taiwan, R.O.C., especially Tse Hung Huang M. D. for his help (MOST 109–2327-B-182–002).

Consent for publication

Not applicable (not contain any individual person's data).

Authors' contributions

Ching-Yuan Wu conceived the idea and designed experiments and analyzed the data and Ming-Shao Tsai wrote manuscript. Yu-Shih Lin, Li-Hsin Shu, Yu-Ching Cheng and Hung-Te Liu performed the experiments; Wei-Tai Shih, Yao-Hsu Yang and Geng-He Chang analyzed the data; Cheng-Ming Hsu, Reming-Albert Yeh revised the manuscript. Rou-Chen Shen, Yu-Huei Wu and Yu-Heng Wu revised the English writing. All authors reviewed and approved the final version.

References

[1] A.C. Walls, Y.J. Park, M.A. Tortorici, A. Wall, A.T. McGuire, D. Veesler, Structure, function, and antigenicity of the SARS-CoV-2 spike glycoprotein, Cell (2020).
[2] R. Yan, Y. Zhang, Y. Li, L. Xia, Y. Guo, Q. Zhou, Structural basis for the recognition of the SARS-CoV-2 by full-length human ACE2, Science (2020).
[3] M. Hoffmann, H. Kleine-Weber, S. Schroeder, N. Kruger, T. Herrler, S. Erichsen, T. S. Schiergens, G. Herrler, N.H. Wu, A. Nitsche, M.A. Muller, C. Drosten, S. Pohlmann, SARS-CoV-2 cell entry depends on ACE2 and TMPRSS2 and is blocked by a clinically proven protease inhibitor, Cell (2020).
[4] S. Duffy, Why are RNA virus mutation rates so damn high? PLoS Biol. 16 (8) (2018), e3000003.
[5] Q. Li, J. Wu, J. Nie, L. Zhang, H. Hao, S. Liu, C. Zhao, Q. Zhang, H. Liu, L. Nie, H. Qin, M. Wang, Q. Lu, X. Li, Q. Sun, J. Liu, L. Zhang, X. Li, W. Huang, Y. Wang, The impact of mutations in SARS-CoV-2 Spike on viral infectivity and antigenicity, Cell 182 (5) (2020) 1284–1294, e9.
[6] E. Boehm, I. Kronig, R.A. Neher, I. Eckerle, P. Vetter, L. Kaiser, D, Geneva Center for Emerging Viral, Novel SARS-CoV-2 variants: the pandemics within the pandemic, Clin. Microbiol Infect. (2021).
[7] H. Liu, P. Wei, Q. Zhang, Z. Chen, K. Aviszus, W. Downing, S. Peterson, L. Reynoso, G.P. Downey, S.K. Frankel, J. Kappler, P. Marrack, G. Zhang, 501Y.V2 and 501Y.V3 variants of SARS-CoV-2 lose binding to Bamlanivimab in vitro, bioRxiv (2021).
[8] H. Liu, P. Wei, Q. Zhang, Z. Chen, K. Aviszus, W. Downing, S. Peterson, L. Reynoso, G.P. Downey, S.K. Frankel, J. Kappler, P. Marrack, G. Zhang, 501Y.V2 and 501Y.V3 variants of SARS-CoV-2 lose binding to bamlanivimab in vitro, MAbs 13 (1) (2021), 1919285.
[9] C.E. Gomez, B. Perdiguero, M. Esteban, Emerging SARS-CoV-2 variants and impact in global vaccination programs against SARS-CoV-2/COVID-19, in: Vaccines, 9, Basel,, 2021.
[10] P. Wang, M.S. Nair, L. Liu, S. Iketani, Y. Luo, Y. Guo, M. Wang, J. Yu, B. Zhang, P. D. Kwong, B.S. Graham, J.R. Mascola, J.Y. Chang, M.T. Yin, M. Sobieszczyk, C. A. Kyratsous, L. Shapiro, Z. Sheng, Y. Huang, D.D. Ho, Antibody resistance of SARS-CoV-2 variants B.1.351 and B.1.1.7, Nature (2021).
[11] Y.J. Kim, U.S. Jang, S.M. Soh, J.Y. Lee, H.R. Lee, The impact on infectivity and neutralization efficiency of SARS-CoV-2 lineage B.1.351 Pseudovirus, Virus 13 (4) (2021).
[12] L.B. Shrestha, N. Tedla, R.A. Bull, Broadly-neutralizing antibodies against emerging SARS-CoV-2 variants, Front. Immunol. 12 (2021), 752003.
[13] M. Li, F. Lou, H. Fan, SARS-CoV-2 Variants of Concern Delta: a great challenge to prevention and control of COVID-19, Signal Transduct. Target Ther. 6 (1) (2021) 349.
[14] L. Queiros-Reis, P. Gomes da Silva, J. Goncalves, A. Brancale, M. Bassetto, J. R. Mesquita, SARS-CoV-2 virus-host interaction: currently available structures and implications of variant emergence on infectivity and immune response, Int. J. Mol. Sci. 22 (19) (2021).
[15] C.Y. Wu, Y.S. Lin, Y.H. Yang, L.H. Shu, Y.C. Cheng, H.T. Liu, Potential simultaneous inhibitors of angiotensin-converting enzyme 2 and transmembrane protease, serine 2, Front. Pharm. 11 (2020), 584158.
[16] A. Carino, F. Moraca, B. Fiorillo, S. Marchiano, V. Sepe, M. Biagioli, C. Finamore, S. Bozza, D. Francisci, E. Distrutti, B. Catalanotti, A. Zampella, S. Fiorucci, Hijacking SARS-CoV-2/ACE2 receptor interaction by natural and semi-synthetic steroidal agents acting on functional pockets on the receptor binding domain, Front. Chem. 8 (2020), 572885.
[17] K.K. Chan, D. Dorosky, P. Sharma, S.A. Abbasi, J.M. Dye, D.M. Kranz, A.S. Herbert, E. Procko, Engineering human ACE2 to optimize binding to the spike protein of SARS coronavirus 2, Science 369 (6508) (2020) 1261–1265.
[18] M. Letko, A. Marzi, V. Munster, Functional assessment of cell entry and receptor usage for SARS-CoV-2 and other lineage B betacoronaviruses, Nat. Microbiol 5 (4) (2020) 562–569.
[19] S. Ozono, Y. Zhang, H. Ode, K. Sano, T.S. Tan, K. Imai, K. Miyoshi, S. Kishigami, T. Ueno, Y. Iwatani, T. Suzuki, K. Tokunaga, SARS-CoV-2 D614G spike mutation increases entry efficiency with enhanced ACE2-binding affinity, Nat. Commun. 12 (1) (2021) 848.
[20] A. Khan, T. Zia, M. Suleman, T. Khan, S.S. Ali, A.A. Abbasi, A. Mohammad, D. Q. Wei, Higher infectivity of the SARS-CoV-2 new variants is associated with K417N/T, E484K, and N501Y mutants: an insight from structural data, J. Cell Physiol. (2021).
[21] J.D. Pedelacq, S. Cabantous, T. Tran, T.C. Terwilliger, G.S. Waldo, Engineering and characterization of a superfolder green fluorescent protein, Nat. Biotechnol. 24 (1) (2006) 79–88.
[22] N.R. Faria, T.A. Mellan, C. Whittaker, I.M. Claro, D.D.S. Candido, S. Mishra, M.A. E. Crispim, F.C.S. Sales, I. Hawryluk, J.T. McCrone, R.J.G. Hulswit, L.A.M. Franco, M.S. Ramundo, J.G. de Jesus, P.S. Andrade, T.M. Coletti, G.M. Ferreira, C.A. M. Silva, E.R. Manuli, R.H.M. Pereira, P.S. Peixoto, M.U.G. Kraemer, N. Gaburo Jr., C.D.C. Camilo, H. Hoeltgebaum, W.M. Souza, E.C. Rocha, L.M. de Souza, M.C. de Pinho, L.J.T. Araujo, F.S.V. Malta, A.B. de Lima, J.D.P. Silva, D.A.G. Zauli, A.C. S. Ferreira, R.P. Schnekenberg, D.J. Laydon, P.G.T. Walker, H.M. Schluter, A.L. P. Dos Santos, M.S. Vidal, V.S. Del Caro, R.M.F. Filho, H.M. Dos Santos, R. S. Aguiar, J.L. Proenca-Modena, B. Nelson, J.A. Hay, M. Monod, X. Miscouridou, H. Coupland, R. Sonabend, M. Vollmer, A. Gandy, C.A. Prete Jr., V.H. Nascimento, M.A. Suchard, T.A. Bowden, S.L.K. Pond, C.H. Wu, O. Ratmann, N.M. Ferguson, C. Dye, N.J. Loman, P. Lemey, A. Rambaut, N.A. Fraiji, M. Carvalho, O.G. Pybus,

S. Flaxman, S. Bhatt, E.C. Sabino, , Genomics and epidemiology of the P.1 SARS-CoV-2 lineage in Manaus, Brazil, Science 372 (6544) (2021) 815–821.
[23] K. Tao, P.L. Tzou, J. Nouhin, R.K. Gupta, T. de Oliveira, S.L. Kosakovsky Pond, D. Fera, R.W. Shafer, The biological and clinical significance of emerging SARS-CoV-2 variants, Nat. Rev. Genet. (2021).
[24] X. Zhu, D. Mannar, S.S. Srivastava, A.M. Berezuk, J.P. Demers, J.W. Saville, K. Leopold, W. Li, D.S. Dimitrov, K.S. Tuttle, S. Zhou, S. Chittori, S. Subramaniam, Cryo-electron microscopy structures of the N501Y SARS-CoV-2 spike protein in complex with ACE2 and 2 potent neutralizing antibodies, PLoS Biol. 19 (4) (2021), e3001237.
[25] H. Liu, Q. Zhang, P. Wei, Z. Chen, K. Aviszus, J. Yang, W. Downing, S. Peterson, C. Jiang, B. Liang, L. Reynoso, G.P. Downey, S.K. Frankel, J. Kappler, P. Marrack, G. Zhang, The basis of a more contagious 501Y.V1 variant of SARS-COV-2, bioRxiv (2021).
[26] H. Liu, Q. Zhang, P. Wei, Z. Chen, K. Aviszus, J. Yang, W. Downing, C. Jiang, B. Liang, L. Reynoso, G.P. Downey, S.K. Frankel, J. Kappler, P. Marrack, G. Zhang, The basis of a more contagious 501Y.V1 variant of SARS-CoV-2, Cell Res. 31 (6) (2021) 720–722.
[27] T.N. Starr, A.J. Greaney, S.K. Hilton, D. Ellis, K.H.D. Crawford, A.S. Dingens, M. J. Navarro, J.E. Bowen, M.A. Tortorici, A.C. Walls, N.P. King, D. Veesler, J. D. Bloom, Deep mutational scanning of SARS-CoV-2 receptor binding domain reveals constraints on folding and ACE2 binding, Cell 182 (5) (2020) 1295–1310, e20.
[28] H. Gu, Q. Chen, G. Yang, L. He, H. Fan, Y.Q. Deng, Y. Wang, Y. Teng, Z. Zhao, Y. Cui, Y. Li, X.F. Li, J. Li, N.N. Zhang, X. Yang, S. Chen, Y. Guo, G. Zhao, X. Wang, D.Y. Luo, H. Wang, X. Yang, Y. Li, G. Han, Y. He, X. Zhou, S. Geng, X. Sheng, S. Jiang, S. Sun, C.F. Qin, Y. Zhou, Adaptation of SARS-CoV-2 in BALB/c mice for testing vaccine efficacy, Science 369 (6511) (2020) 1603–1607.
[29] C. Laffeber, K. de Koning, R. Kanaar, J. Hg Lebbink, Experimental evidence for enhanced receptor binding by rapidly spreading SARS-CoV-2 variants, J. Mol. Biol. (2021), 167058.
[30] B.O. Villoutreix, V. Calvez, A.G. Marcelin, A.M. Khatib, In silico investigation of the New UK (B.1.1.7) and South African (501Y.V2) SARS-CoV-2 variants with a focus at the ACE2-Spike RBD interface, Int. J. Mol. Sci. 22 (4) (2021).
[31] D. Focosi, F. Maggi, Neutralising antibody escape of SARS-CoV-2 spike protein: risk assessment for antibody-based Covid-19 therapeutics and vaccines, Rev. Med Virol. (2021).
[32] A. Khan, T. Zia, M. Suleman, T. Khan, S.S. Ali, A.A. Abbasi, A. Mohammad, D. Q. Wei, Higher infectivity of the SARS-CoV-2 new variants is associated with K417N/T, E484K, and N501Y mutants: an insight from structural data, J. Cell Physiol. 236 (10) (2021) 7045–7057.
[33] R. Pompei, O. Flore, M.A. Marccialis, A. Pani, B. Loddo, Glycyrrhizic acid inhibits virus growth and inactivates virus particles, Nature 281 (5733) (1979) 689–690.
[34] L. Diomede, M. Beeg, A. Gamba, O. Fumagalli, M. Gobbi, M. Salmona, Can Antiviral activity of licorice help fight COVID-19 infection? Biomolecules 11 (6) (2021).
[35] X. Sui, J. Yin, X. Ren, Antiviral effect of diammonium glycyrrhizinate and lithium chloride on cell infection by pseudorabies herpesvirus, Antivir. Res 85 (2) (2010) 346–353.
[36] C. Feng Yeh, K.C. Wang, L.C. Chiang, D.E. Shieh, M.H. Yen, J. San Chang, Water extract of licorice had anti-viral activity against human respiratory syncytial virus in human respiratory tract cell lines, J. Ethnopharmacol. 148 (2) (2013) 466–473.
[37] S.K. Sinha, S.K. Prasad, M.A. Islam, S.K. Chaudhary, S. Singh, A. Shakya, Potential leads from liquorice against SARS-CoV-2 main protease using molecular docking simulation studies, Comb. Chem. High. Throughput Screen 24 (4) (2021) 591–597.
[38] V. Srivastava, A. Yadav, P. Sarkar, Molecular docking and ADMET study of bioactive compounds of glycyrrhiza glabra against main protease of SARS-CoV2, Mater. Today Proc. (2020).
[39] L. van de Sand, M. Bormann, M. Alt, L. Schipper, C.S. Heilingloh, E. Steinmann, D. Todt, U. Dittmer, C. Elsner, O. Witzke, A. Krawczyk, Glycyrrhizin effectively inhibits SARS-CoV-2 replication by inhibiting the viral main protease, Viruses 13 (4) (2021).
[40] X. Li, Q. Qiu, M. Li, H. Lin, S. Cao, Q. Wang, Z. Chen, W. Jiang, W. Zhang, Y. Huang, H. Luo, L. Luo, Chemical composition and pharmacological mechanism of ephedra-glycyrrhiza drug pair against coronavirus disease 2019 (COVID-19), Aging 13 (4) (2021) 4811–4830.
[41] S.K. Sinha, S.K. Prasad, M.A. Islam, S.S. Gurav, R.B. Patil, N.A. AlFaris, T. S. Aldayel, N.M. AlKehayez, S.M. Wabaidur, A. Shakya, Identification of bioactive compounds from Glycyrrhiza glabra as possible inhibitor of SARS-CoV-2 spike glycoprotein and non-structural protein-15: a pharmacoinformatics study, J. Biomol. Struct. Dyn. (2020) 1–15.
[42] J. Li, D. Xu, L. Wang, M. Zhang, G. Zhang, E. Li, S. He, Glycyrrhizic acid inhibits SARS-CoV-2 infection by blocking spike protein-mediated cell attachment, Molecules 26 (20) (2021).
[43] Z. Zhao, Y. Xiao, L. Xu, Y. Liu, G. Jiang, W. Wang, B. Li, T. Zhu, Q. Tan, L. Tang, H. Zhou, X. Huang, H. Shan, Glycyrrhizic acid nanoparticles as antiviral and anti-inflammatory agents for COVID-19 treatment, ACS Appl. Mater. Interfaces 13 (18) (2021) 20995–21006.
[44] V.V. Fomenko, N.B. Rudometova, O.I. Yarovaya, A.D. Rogachev, A.A. Fando, A. V. Zaykovskaya, N.I. Komarova, D.N. Shcherbakov, O.V. Pyankov, A.G. Pokrovsky, L.I. Karpenko, R.A. Maksyutov, N.F. Salakhutdinov, Synthesis and in vitro study of antiviral activity of glycyrrhizin nicotinate derivatives against HIV-1 pseudoviruses and SARS-CoV-2 viruses, Molecules 27 (1) (2022).
[45] E. Ohgitani, M. Shin-Ya, M. Ichitani, M. Kobayashi, T. Takihara, M. Kawamoto, H. Kinugasa, O. Mazda, Significant inactivation of SARS-CoV-2 in vitro by a green tea catechin, a catechin-derivative, and black tea galloylated theaflavins, Molecules 26 (12) (2021).
[46] J. Lung, Y.S. Lin, Y.H. Yang, Y.L. Chou, L.H. Shu, Y.C. Cheng, H.T. Liu, C.Y. Wu, The potential chemical structure of anti-SARS-CoV-2 RNA-dependent RNA polymerase, J. Med Virol. (2020).